Current Research in Insect Science 3 (2023) 100062

Contents lists available at ScienceDirect

Current Research in Insect Science

journal homepage: www.elsevier.com/locate/cris

Structure of an antennally-expressed carboxylesterase suggests lepidopteran odorant degrading enzymes are broadly tuned

Jacob A. Corcoran[a,d,*], Cyril Hamiaux[b], Nicoletta Faraone[c,d], Christer Löfstedt[d], Colm Carraher[b,d]

[a] USDA - Agricultural Research Service, Biological Control of Insects Research Laboratory, Columbia, MO, USA
[b] The New Zealand Institute for Plant and Food Research Limited, Auckland, New Zealand
[c] Department of Chemistry, Acadia University, Wolfville, Nova Scotia, Canada
[d] Department of Biology, Lund University, Lund, Sweden

ARTICLE INFO

Keywords:
Epiphyas postvittana
Carboxyl/cholinesterase
Odorant degrading enzyme
RNAseq
GC-MS
Crystal structure

ABSTRACT

Insects rely on the detection of chemical cues present in the environment to guide their foraging and reproductive behaviour. As such, insects have evolved a sophisticated chemical processing system in their antennae comprised of several types of olfactory proteins. Of these proteins, odorant degrading enzymes are responsible for metabolising the chemical cues within the antennae, thereby maintaining olfactory system function. Members of the carboxyl/cholinesterase gene family are known to degrade odorant molecules with acetate-ester moieties that function as host recognition cues or sex pheromones, however, their specificity for these compounds remains unclear. Here, we evaluate expression levels of this gene family in the light-brown apple moth, *Epiphyas postvittana,* via RNAseq and identify putative odorant degrading enzymes. We then solve the apo-structure for EposCCE24 by X-ray crystallography to a resolution of 2.43 Å and infer substrate specificity based on structural characteristics of the enzyme's binding pocket. The specificity of EposCCE24 was validated by testing its ability to degrade biologically relevant and non-relevant sex pheromone components and plant volatiles using GC–MS. We found that EposCCE24 is neither capable of discriminating between linear acetate-ester odorant molecules of varying chain length, nor between molecules with varying double bond positions. EposCCE24 efficiently degraded both plant volatiles and sex pheromone components containing acetate-ester functional groups, confirming its role as a broadly-tuned odorant degrading enzyme in the moth olfactory organ.

1. Introduction

The world, to an insect, must "look" like an incredibly thick wall of smells, for as insects navigate their environment they are inundated with thousands of volatile odorant compounds that are constantly being emitted by microorganisms, plants and other animals. While the vast majority of these compounds carry no "message" that is of interest to a given insect, others carry information that is of critical importance to its survival. In this case, the insect has evolved to depend on these biologically relevant messages to locate mates, find food, or lay eggs, *in real time*. For this to occur, insects rely on an extraordinarily sensitive and highly efficient odorant processing system comprised of olfactory proteins, each with a distinct role in filtering critical odorant messengers out from a huge collection of environmental noise (reviewed in Leal, 2013).

All of the volatile chemical cues present in the environment travel through air until they are degraded by the elements or by an organism's chemosensory system. If these molecules encounter an insect before degradation, they may passively enter small pores present in hairs called sensilla that line the length of the insect's antennae. Within these sensilla reside odorant receptors (ORs) embedded in the membranes of olfactory sensory neurons (OSNs) which are submerged in an aqueous lymph (Carey and Carlson, 2011). Because volatile odorant compounds tend to be hydrophobic, the aqueous lymph within the sensilla functions as a molecular sieve, preventing uncontrolled flooding of the olfactory organ with external chemical messages. The current model suggests that certain odorant molecules are selectively picked up by soluble carrier proteins (*e.g.*, odorant binding proteins, OBPs) present in the sensillar lymph and transported to the ORs present in the OSNs (Chang et al., 2015; Forstner et al., 2009; Leal, 2013; Xu et al., 2005). Evidence sug-

* Corresponding author at: USDA – Agricultural Research Service, Biological Control of Insects Research Laboratory, 1503 S. Providence Road, Columbia, MO 65203, USA.
E-mail address: Jacob.corcoran@usda.gov (J.A. Corcoran).

https://doi.org/10.1016/j.cris.2023.100062
Received 8 February 2023; Received in revised form 1 June 2023; Accepted 2 June 2023

gests that odorant-OBP complexes then undergo a pH-induced conformational change as they approach the OSNs and release the odorant molecule to interact with and activate the OR (Leal et al., 2005). Olfactory receptor activation subsequently causes the depolarisation of the OSN, sending a stimulus to the brain to be interpreted and acted upon. Also present in the sensillar lymph are odorant degrading enzymes (ODEs), which effectively act as tenacious scavengers, metabolising free odorant molecules and thus preventing saturation of the olfactory system (Ishida and Leal, 2005).

Insects possess several classes of ODEs, such as aldehyde-oxidases (AOXs) (Choo et al., 2013), aldehyde-dehydrogenases (Leal and Barbancho 1993), carboxyl/cholinesterases (CCEs) (Chertemps et al., 2012) and hydrolases (*e.g.*, cytochrome p450s) (Maibeche-Coisne et al., 2004a), with each class containing numerous proteins that display high sequence diversity (Vogt, 2005). However, because non-odorant compounds may also contain the molecular moieties that these various enzyme classes act upon (*e.g.*, aldehyde functional groups), it is important to consider olfactory organ expression levels when considering olfactory protein family diversity within an organism. For example, in the silkworm moth, *Bombyx mori*, 76 different CCEs were identified within its genome, however only 36 of these were found to be expressed in the moth's antennae (Qiu et al., 2018). A specific subset of antennally-expressed ODEs, regardless of the molecular moieties they act upon, are commonly referred to as pheromone degrading enzymes (PDEs), either only conceptually or because a given ODE was found to degrade a biologically relevant pheromone compound *in vitro* (*e.g.,* Ishida and Leal, 2005).

Considering the chemical structure of semiochemicals present in the environment, a large proportion contain acetate-ester functional groups (www.pherobase.com). Lepidopteran insects, which typically rely on detecting (and therefore, degrading) long, acetate-ester containing hydrocarbons for reproductive and foraging purposes, usually express several CCEs in their antennae. However, unlike the relatively large body of data that describes the interactions of acetate-ester compounds with lepidopteran ORs and OBPs, to date only nine lepidopteran CCEs have been tested for their ability to interact with plant volatiles and/or sex pheromone compounds, with one being from the silkworm moth, *Antheraea polyphemus* (Ishida and Leal, 2005), five from the beet armyworm, *Spodoptera exigua* (He et al., 2014a,b,c, 2015, 2020), two from the African cotton leafworm, *S. littoralis* (Durand et al., 2010, 2011), and one from the tobacco cutworm, *S. littura* (He et al., 2014c). Of these functionally characterised lepidopteran CCEs, five were tested for their ability to degrade biologically relevant (*i.e.,* sex pheromone) compounds only, while the other four were tested against biologically relevant as well as other structurally-related volatile odorants. While it is difficult to evaluate the true specificity of those CCEs tested only against specific sex pheromone components, the results from those tested against panels of compounds found most to be broadly tuned, degrading sex pheromone components and plant volatiles, biologically relevant or not. Interestingly, SexiCCE10 was the only CCE found to be somewhat specific when tested against a broad panel of compounds, being able to degrade various plant volatiles but not sex pheromone components (He et al., 2015). Therefore, the currently available data suggest that lepidopteran CCEs are likely to be broadly tuned; whether or not this holds true for all CCEs or other ODE classes remains to be determined.

To date, very few insect esterase enzymes have had their structures solved (Wogulis et al., 2006; Jackson et al., 2013; Han et al., 2018; Younus et al., 2017; Hopkins et al., 2017; Harel et al., 2000). However, those that have, coupled with sequence-level analyses and protein modelling, do provide insight into general overarching elements of these enzymes. For example, despite sharing relatively low sequence identities (~30–35%) the different insect esterase structures superimpose well over a canonical α/β hydrolase fold consisting of a core, 8-stranded β-sheet surrounded by 6 α-helices. This core structure is further extended by the presence of additional small antiparallel strands on both sides of the β-sheet and by two mostly α-helical, more divergent, subdomains protruding above the β-sheet that contribute to the formation of the substrate binding pocket and the active site entrance that leads to the conserved catalytic triad and oxyanion hole. The sizes and shapes of the substrate binding pockets generally reflect the various substrates of the insect esterases solved to date: acetylcholine (AgamAChE-1, Han et al., 2018 and DmelAChE-2, Harel et al., 2000), juvenile hormone (MsexJHE, Wogulis et al., 2006), short- to mid-chain food esters (DmelEst6, Younus et al., 2017), fatty acid methyl esters (LcupαE7, Jackson et al., 2013), and mono and diacylglycerols (CquiEstβ2, Hopkins et al., 2017).

The aim of the current study is to identify and characterise a pheromone-degrading CCE from the light-brown apple moth, *Epiphyas postvittana*, a horticultural pest native to Australia that has subsequently spread globally (Tooman et al., 2011). Due to the critical role that olfactory proteins play in insect foraging and reproductive biology, coupled with their evolutionary uniqueness, these proteins are widely touted as being ideal targets for the development of next-generation insecticides (Andersson and Newcomb, 2017; Venthur and Zhou, 2018). However, the focus of this study is to address the question of whether the CCE is specifically tuned to the acetate-ester sex pheromone components used by this species (El-Sayed et al., 2011) or if it is capable of degrading a wider range of acetates. Towards this end, we first deployed a bioinformatic approach to evaluate the expression of the CCE gene family in the antennae of this species, as well as their phylogenetic relatedness to functionally characterised CCEs from other moths. Based on these data, we selected one CCE as being a putative pheromone degrading enzyme and solved its 3-dimensional structure by crystallographic analysis to determine if substrate specificity can be inferred based on structural properties. Finally, we evaluated our structurally-based prediction of CCE specificity by testing the ability of a recombinant version of the protein to degrade various acetate-ester-containing odorant molecules, including biologically relevant plant volatiles and sex pheromone components.

2. Methods & materials

2.1. Transcriptomic sequencing & gene expression analyses

Male and female *E. postvittana* were obtained from a colony maintained at the New Zealand Institute for Plant and Food Research Ltd., Auckland, New Zealand. Two- to three-day old adult male and female moths were snap frozen in liquid nitrogen after which heads, antennae and wings were removed from bodies and used to prepare three pools (each) of the following: 30 pairs of male antennae, 30 pairs of female antennae, 3 male bodies and 3 female bodies. Total RNA was extracted from each of the 12 tissue samples using Trizol (ThermoFisher, Waltham, MA, USA) reagent according to the manufacturer's protocol and stored at −80 °C. The 12 RNA samples were then shipped to Novogene (Sacramento, CA, USA) for sample quality analysis, library preparation, sequencing using Illumina's NovaSeq (PE150) technology, transcriptome assembly and transcript expression analyses. Raw sequencing data were filtered to remove low-quality reads and adapter sequences prior to *de novo* transcriptome assembly using Trinity software v2.6.6 (Grabherr et al., 2011) software. Clean reads were then mapped onto the transcriptome using RSEM software v1.2.28 (Li and Dewey, 2011) for gene expression analyses. Readcounts were normalized amongst biological replicates using DESeq2 software v1.26.0 (Love et al., 2014) to identify differentially expressed genes between tissue samples. Carboxylesterases were manually identified and annotated within the transcriptome using the sequences of *E. postvittana* carboxylesterases previously identified from a draft genome and antennal transcriptome (Corcoran et al., 2015) and were deemed to be differentially expressed between tissue samples if the $\log_2$(fold change) was greater than 1 and the adjusted p-value was less than 0.05.

2.2. Phylogenetics

Sequences of lepidopteran carboxylesterases with validated antennal expression, including those identified in the transcriptome produced in this study, were used in phylogenetic analyses to identify EposCCEs closely related to other lepiodopteran CCEs that had previously been shown to degrade sex pheromone compounds. Amino acid sequences encoding CCEs from *Bombyx mori* (Qiu et al., 2018), *Spodoptera exigua* (He et al., 2014a, 2014b), *S. littoralis* (Durand et al., 2010, 2012; Walker et al., 2019), *S. litura* (He et al., 2014c), *Antherea polyphemus* (Ishida and Leal, 2002, 2005), *Sesamia nonagrioides* (Merlin et al., 2007) and *Mamestra brassicae* (Maibeche-Coisne et al., 2004b) were used along with EposCCEs that displayed male or female antennal expression to produce a multiple sequence alignment using the MUSCLE application embedded in Geneious software v2022.2.2 (Biomatters Ltd., Auckland, New Zealand). The resulting sequence alignment was then used to construct a phylogenetic tree using PhyML software based on 1000 bootstrap replicates. The presence of N-terminal signal peptides, which indicate the ability of the protein to be secreted extracellularly, were predicted for all 133 CCEs included in the phylogenetic analysis using SignalP-6.0 (www. services.healthtech.dtu.dk).

2.3. Protein production

The C-terminally His_{10}-tagged EposCCE24 construct was synthesised (Genscript, Piscataway, NJ, USA), gateway cloned into the pDEST8 vector and transformed into DH10Bac cells as per the manufacturer's protocol. Bacmids were purified according to the Bac-to-Bac manual and transfected into Sf9 cells to generate high-titre virus stocks. Hi5 cells (*Trichoplusia ni*) at 1×10^6 cells/mL were infected with virus at an MOI of 1 and incubated at 27 °C with shaking at 120 RPM for 72 h. The cells were centrifuged at 8000 x *g* for 20 min, and the supernatant was passed through a 0.22 μm filter prior to being applied to a 5 mL NiNTA Excel column (Cytiva, Marlborough, MA, USA). The column was washed with 10 column volumes of buffer A (20 mM Tris/HCl pH 8, 300 mM NaCl) with 20 mM imidazole followed by 10 column volumes of buffer A with 50 mM imidazole, and eluted with 5 column volumes of buffer A with 500 mM imidazole. The His_{10} tag was removed by cleavage with TEV enzyme. The cleaved protein was further purified by size exclusion chromatography using a superdex 200 16/60 column (Cytiva, Marlborough, MA, USA) in buffer A. Peak fractions were collected and concentrated to 15–17 mg/mL and frozen at −80 °C until use in functional experiments or crystallisation screens.

2.4. Crystallisation

Crystallisation experiments were performed by hanging drop vapour diffusion at 20 °C. The sparse-matrix screens JCSG-plus, MIDAS-plus, Structure Screen 1 + 2 and MORPHEUS (Molecular Dimensions, Rotherham, United Kingdom) were used as 200 μL reservoir solutions in 96-well flat-bottom plates. Drops consisting of 1 μL EposCCE24 at 15–17 mg/mL and 1 μL reservoir solution were dispensed manually on a qPCR film (UC-500, Corning, Tewksbury, MA, USA), which was then turned over and sealed on top of the reservoirs. Drops were checked regularly over a 6-month period. Crystals were successfully grown in the Midas screen under the following conditions, 0.1 M Tris pH 8.5, 25% w/v SOKALAN® CP 5, and were further refined with 27.5% SOKALAN® CP 5, 0.1 M Tris pH 8, using a protein concentration of 8.5 mg/mL.

2.5. Structure determination

Crystals were soaked in mother liquor containing 25% glycerol and snap frozen in liquid nitrogen. Datasets were collected at the MX1 and MX2 beamlines of the Australian synchrotron (Melbourne, Australia). The majority of crystals belong to either monoclinic or orthorhombic space groups and showed weak diffraction patterns, rarely extending beyond 3.1 Å resolution. All datasets were indexed and integrated with XDS (Kabsch, 2010), and scaled/merged with Aimless (Evans and Murshudov, 2013) from the CCP4 suite (Winn et al., 2011). The structure was initially solved by molecular replacement with MorDa (Vagin and Lebedev, 2015) on the CCP4-online server using one orthorhombic dataset diffracting to 3.3 Å resolution. Crystals belong to the $P2_12_12_1$ space group, with cell parameters a=119.60, b=168.37, c=246.40 Å and 8 molecules per asymmetric unit. The starting model identified by MorDa was esterase 6 from *Drosophila melanogaster* (DmelEst6; PDB entry: 5THM) that shares ~32% sequence identity with EposCCE24. An EposCCE24 model was subsequently built with Autobuild and partially refined with Phenix.refine (Liebschner et al., 2019).

Among all the datasets collected, a 2.43 Å resolution dataset was obtained from a unique crystal belonging to the P1 space group. Morphologically, this crystal was indistinguishable from any other crystals grown in similar conditions. Statistics for data collection and processing are listed in Table S1. The structure was solved by molecular replacement using one monomer of the partially refined model of EposCCE24 as a starting model in Molrep from the CCP4. As in the previous orthorhombic crystal form, 8 molecules are present in the asymmetric unit of the triclinic crystal form, although the organization of the 8 monomers in the asymmetric unit is completely different between the two crystal forms. Subsequent cycles of model building and refinement were performed in Coot (Emsley et al., 2010) and Refmac5 (Murshudov et al., 2011), respectively. Clear electron density was observed for carbohydrate chains consisting of 5 monomers (NAG-NAG-BMA-MAN-MAN) attached to Asn438 of each molecule of the asymmetric unit. The refinement statistics are listed in Table S2.

2.6. Docking

3D coordinates for compounds were obtained from PubChem in sdf format and converted into the pdbqt format using OpenBabel (O'Boyle et al., 2011) and AutoDockTools (Morris et al., 2009). The EposCCE24 monomer A was prepared for docking by adding polar hydrogens and Gasteiger charges in AutoDockTools. Docking was performed in Autodock Vina (Trott and Olson, 2010) using a $22 \times 11 \times 11$ $Å^3$ box centred on (x=13.56, y=3.25, z=4.75).

2.7. Functional testing

The ability of recombinant EposCCE24 to degrade various acetate-ester sex pheromone compounds and plant odorants, including most of those known to be electrophysiologically active on *E. postvittana* antennae (Suckling et al., 1996; Roh and Park 2022), was determined through an evaluation of substrate degradation by GC–MS. All test compounds and the internal standard, tetradecane, were purchased from commercial suppliers and had purities ranging from 93 to 99%. In these experiments purified, recombinant EposCCE24 was incubated with candidate substrates and the internal standard after which the test compound substrates, products and internal standards were extracted for GC–MS analyses. More specifically, 100 mM stocks of the internal standard and test compounds prepared in 95% ethanol were diluted to a final concentration of 62.5 μM and 125 μM, respectively, in 50 μL of Tris buffer, after which 1 μL of a 1.02 μM solution of EposCCE24 (final concentration of 20 nM) or buffer control was added to the reaction and allowed to incubate for 5 min at 28 °C. A total of six reactions were prepared for each test compound (three with EposCCE24, three with vehicle control). Following incubation, 100 μL of heptane was added to each reaction which was vortexed for 15 s, then centrifuged for 3 min at 2500 x *g* at 4 °C, after which 50 μL was removed from the upper organic layer for GC–MS analysis.

Quantification of test compound degradation by EposCCE24 was carried out on an Agilent 7890A gas chromatography system with an HP-5 capillary column (5% pH-/95% Me-SiO; 30 m, 0.25 mm id; d_f 0.25 μm;

Agilent) equipped with an Agilent 7693 autosampler (splitless injection), interfaced to an Agilent 5975C mass spectrometer. The GC conditions were as follows: injection at 80 ˚C, hold for 1 min, 10 ˚C /min up to 240 ˚C, and a 5 min hold at this temperature. The temperature of the injector and detector were 250 ˚C and 280 ˚C, respectively, and the electronic impact was 70 eV. The area under the curve (AUC) of the resulting peaks for the internal standard and the acetate test compounds was determined in each reaction using the Agilent software. The AUC values for the remaining substrate were normalised to the AUC of the internal standard in each reaction to control for extraction efficiency. The mean normalised AUC was calculated for the three (-) EposCCE24 (*i.e.*, vehicle control) reactions and was compared to the mean normalised AUC for the three (+) EposCCE24 reactions to calculate the percent substrate remaining for each EposCCE24/test compound combination. The K_m and V_{max} of EposCCE24 degradation of two compounds, *(E)*−11-tetradecenyl acetate (E11–14:OAc) and *(Z)*−11-tetradecenyl acetate (Z11–14:OAc), was determined using the same experimental reaction design described above, except that various concentrations (from 500 μM to 3.9 μM, with two-fold dilutions) of the two test compounds were used in reactions with EposCCE24. The rate of degradation of each of these two compounds by EposCCE24 was determined by converting the normalised percent substrate remaining in each reaction to an absolute value of substrate based on the known initial concentration of substrate present in each reaction and dividing this value by the length of time of the reaction. The experimentally determined degradation rate of EposCCE24 for each concentration of test compound was then used to calculate the V_{max} and K_m of EposCCE24 for E11–14:OAc and Z11–14:OAc using the Michaelis-Menten non-linear fit function embedded in GraphPad Prism software v 9.5.0 (www.graphpad.com).

3. Results

3.1. Carboxylesterase expression patterns

Previously, 39 EposCCEs were identified from a variety of genetic resources (Jordan et al., 2008; Corcoran et al., 2015); the open reading frame sequences of these EposCCEs were corrected and/or extended based on the sequencing data obtained in the current study (Supplementary file S1). In the current study two additional carboxylesterases were identified and named EposCCEs 40 and 41. Of the total 41 EposCCE genes, 37 displayed varying expression levels in either antennae or bodies (Fig. 1A) with some showing statistically significant antennae- or body-biased expression (Fig. 1B). EposCCEs 3, 9, 11 and 13 were not expressed (*i.e.,* normalised readcounts ≥1) in antennae or body tissue, and none of the EposCCEs displayed antennal-specific expression. Of the total 41 EposCCE genes, 35 displayed varying expression levels in either male or female antennae (Fig. 2A). EposCCEs 3, 9, 11, 13, 20 and 40 were not expressed (*i.e.,* normalised readcounts ≥1) in male or female antennae. Of the 35 EposCCEs that were detected in male or female antennae, none displayed statistically significant sex-biased antennal expression patterns (Fig. 2B).

3.2. Phylogenetics

The evolutionary relatedness of antennally-expressed EposCCEs to other lepidopteran carboxylesterases was evaluated through phylogenetic analyses. Of the 35 EposCCEs displaying antennal expression, most were interspersed through the resulting phylogenetic tree, likely displaying orthologous relationships between the proteins and those from other moth species. Some EposCCEs displayed paralogous expansion events amongst the CCEs included in the phylogenetic analyses (*e.g.*, EposCCEs 5, 6, 7, 21, 22, 23, 30, 31 and 32). Twenty of the 35 EposCCEs were predicted to contain N-terminal signal peptides and were evenly distributed in the phylogeny, with the exception of the paralogous expansion event noted above, in which all nine EposCCEs contained signal peptides. EposCCEs 24, 29, and those included in the paralogous expansion noted above reside in clades neighbouring other lepidopteran CCEs that have previously demonstrated an ability to degrade sex pheromone components (Fig. 3). However, EposCCE29 does not have a predicted signal peptide and is likely not present in the sensillum lymph.

3.3. Crystal structure of EposCCE24

The EposCCE24 protein was expressed in High Five cells, secreted into the media, and purified by affinity chromatography. The His_{10} tag was removed with TEV protease and the resulting cleaved protein was further purified by size exclusion chromatography. Crystals were obtained by vapour diffusion using SOKALAN® CP 5 as the precipitating agent and cryo-protected with glycerol. A 2.43 Å resolution dataset was collected at the Australian Synchrotron and the structure was solved by molecular replacement, with eight chains per asymmetric unit. Data collection and refinement statistics are listed in Table S1 and S2, respectively. A DALI search against PDB identified the structure of DmelEst6 as the closest structural homologue of EposCCE24, ahead of other insect carboxylesterases. Indeed, while EposCCE24 adopts the typical α/β hydrolase fold also seen for other insect carboxylesterases, its detailed topology is almost identical to that of DmelEst6 (Younus et al., 2014). The only differences are the addition of ~20 amino acids that form two additional small helices at the C-terminus (different from the C-terminal helix observed in other insect carboxylesterases) and the fact that EposCCE24 lacks the third disulphide bridge (Cys493-Cys514) which is unique to Dmel Esterase 6. Despite sharing only 32% sequence identity, the 3-dimensional structures of EposCCE24 and DmelEst6 are remarkably similar, with an r.m.s.d. of 1.51 Å for 488 out of 534 Cα atoms between the two structures (Fig. 4). Consequently, EposCCE24 has the same divergent cavity entrance as DmelEst6 (formed by loops and helices after β1, β4 and β8), in contrast to the other insect esterases (Younus et al., 2017). Residues forming the catalytic triad (Ser184, His437, Asp315) and the oxyanion hole (Gly105, Gly106, Ala 188) are, as expected, conserved in EposCCE24. The main difference between EposCCE24 and DmelEst6 lies in the characteristics of their respective substrate binding pockets (Fig. 5). Overall, the DmelEst6 binding pocket was found to be smaller than for other insect carboxylesterases (Younus et al., 2014). Its asymmetric shape consists of a main cavity that binds the alcohol leaving group of the ester substrates and of a subsite (shown with an asterisk on Fig. 5) proposed to accommodate the substrate's acyl group. Indeed, structural analyses showed that the DmelEst6 subsite can accommodate up to 6 carbons in length, in agreement with the enzyme showing activity towards formate, acetate, propionate, butyrate, pentanoate and hexanoate esters, while the main cavity accepts leaving alcohol groups of up to ~10 carbons, including aromatic and branched moieties (Younus et al., 2014). In comparison, the main binding cavity of EposCCE24 is even smaller (and more precisely, narrower) than that of DmelEst6 due to the presence of three bulky residues, Phe 442, Phe447 and Tyr116 (Ser450, Asn455 and Asn119 in DmelEst6) that cluster on one side of the cavity (Fig. 5). Furthermore, EposCCE24 lacks the subsite, although all residues shaping the subsite in DmelEst6 are conserved in EposCCE24 (Ala107, Trp217, Phe272, Tyr318, Phe390, His437). among these, the slightly altered positions of Tyr318 and Phe390, together with the substitution of Phe113 by Tyr110 in EposCCE24, are responsible for the closure of the subsite (Fig. 5). Altogether, the closure of the subsite in EposCCE24 strongly suggests that EposCCE24 is likely to favour formate or acetate-esters rather than esters carrying longer acyl groups, while the narrower main cavity indicates a possible preference towards linear rather than cyclic or branched alcohol leaving groups. However, because of its relatively shallow depth (the distance from the hydroxyl group of the catalytic serine to the cavity entrance is ~12–13 Å), it is likely that EposCCE24 is unable to discriminate between esters of various chain lengths or between esters carrying different saturation patterns. Indeed, attempts to dock the two main pheromone components of *E. postvitanna* (E11–14:OAc and Z11–

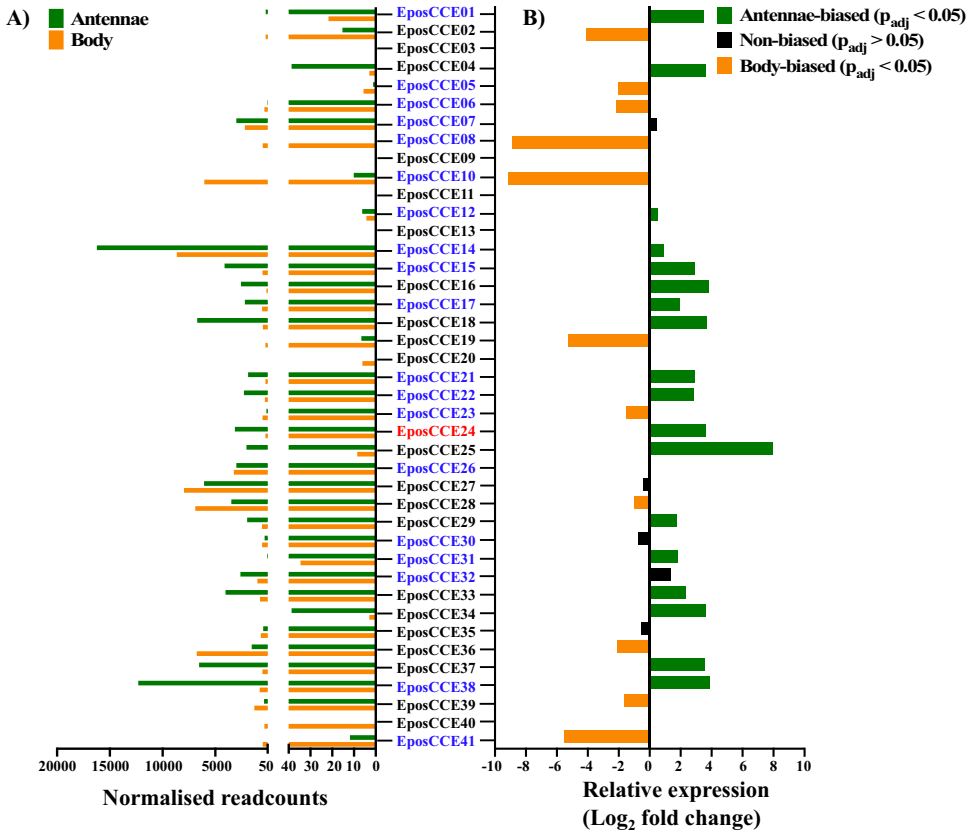

Fig. 1. Carboxyl/cholinesterase (CCE) gene expression in *Epiphyas postvittana* antennae and bodies as determined by RNASeq analyses. A) Normalised readcounts of 41 EposCCE gene transcripts in antennae and bodies. The expression levels of EposCCEs were normalised between six biological replicates (three male and three female, combined) for each tissue type. Note: EposCCEs 3, 9, 11 and 13 are not expressed (normalised readcount >1) in antennae or bodies. B) Relative expression (antennae:body) of EposCCE transcripts present in both antennae and bodies. Note: EposCCEs 20 and 40 are excluded from Fig. 1B due to their lack of expression in antennal tissue samples. Blue or red font indicates predicted extracellular enzymes based on the presence of N-terminal signal peptides (SignalP-6.0).

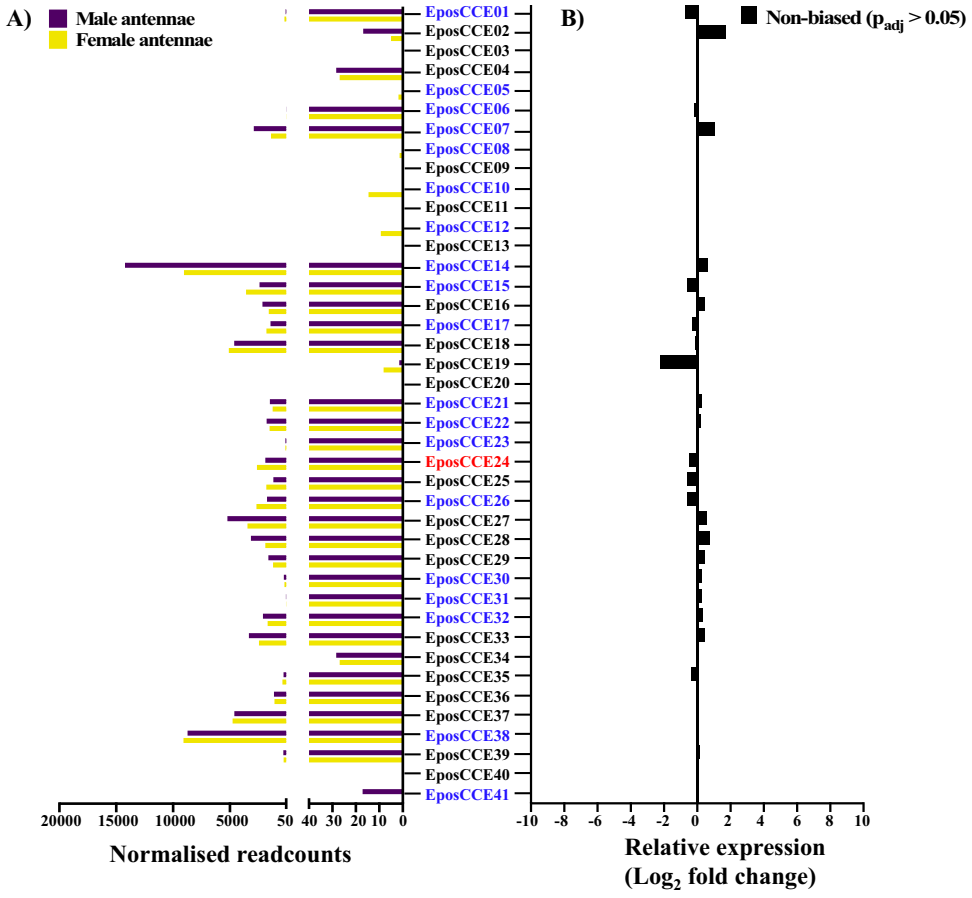

Fig. 2. Carboxyl/cholinesterase (CCE) gene expression in male and female *Epiphyas postvittana* antennae as determined by RNASeq analyses. A) Normalised readcounts of 41 EposCCE transcripts in male and female antennae. The expression levels of EposCCEs were normalised between three biological replicates for each tissue type (male or female antennae). Note: EposCCEs 3, 9, 11, 13, 20 and 40 are not expressed (normalised readcount >1) in male or female antennae. B) Relative expression (male:female) of EposCCE transcripts present in both male and female antennae. Note: EposCCEs 5, 8, 10, 12 and 41 are excluded from Fig. 2B due to their lack of expression in male or female antennal tissue samples. Blue or red font indicates predicted extracellular enzymes based on the presence of N-terminal signal peptides (SignalP-6.0).

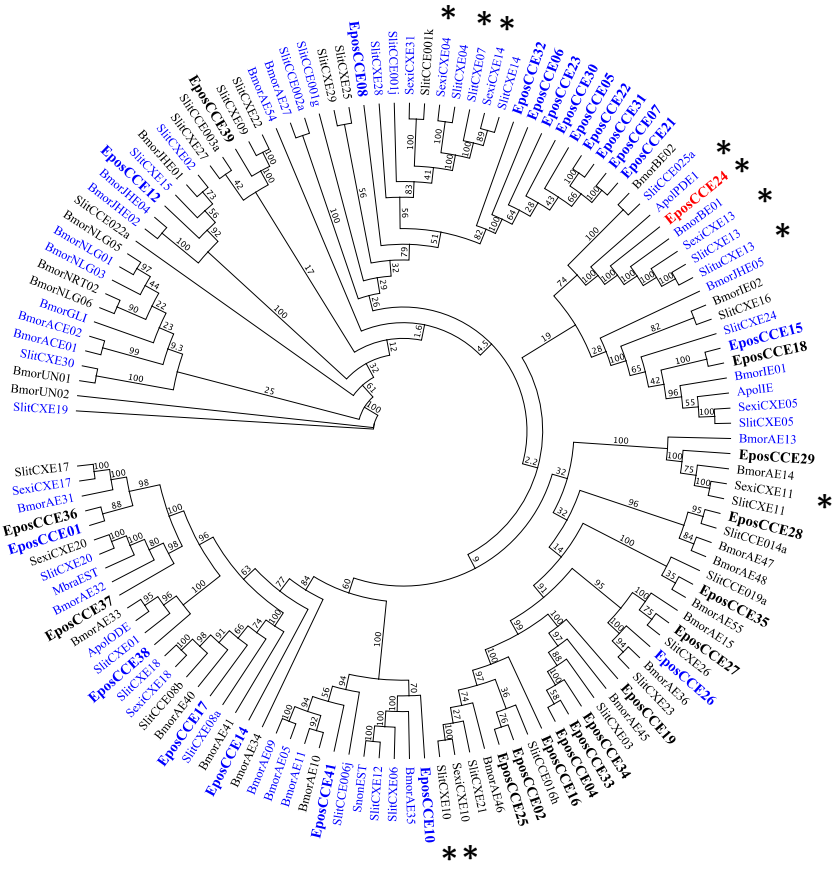

Fig. 3. Lepidopteran carboxyl/cholinesterases with validated antennal expression. Blue or red font indicates predicted extracellular enzymes based on the presence of N-terminal signal peptides (SignalP-6.0). *Epiphyas postvittana* (Epos) genes are shown in bold, large font, and *Bombyx mori* (Bmor), *Spodoptera exigua* (Sexi), *Spodoptera littoralis* (Slit), *Spodoptera litura* (Slitu), *Antherea polyphemus* (Apol), *Sesamia nonagrioides* (Snon) and *Mamestra brassicae* (Mbra) genes are shown in regular, small font. Asterisks indicate genes that have been functionally tested for their ability to degrade sex pheromones and/or plant volatiles. Node values represent bootstrap values based on 1000 replicates.

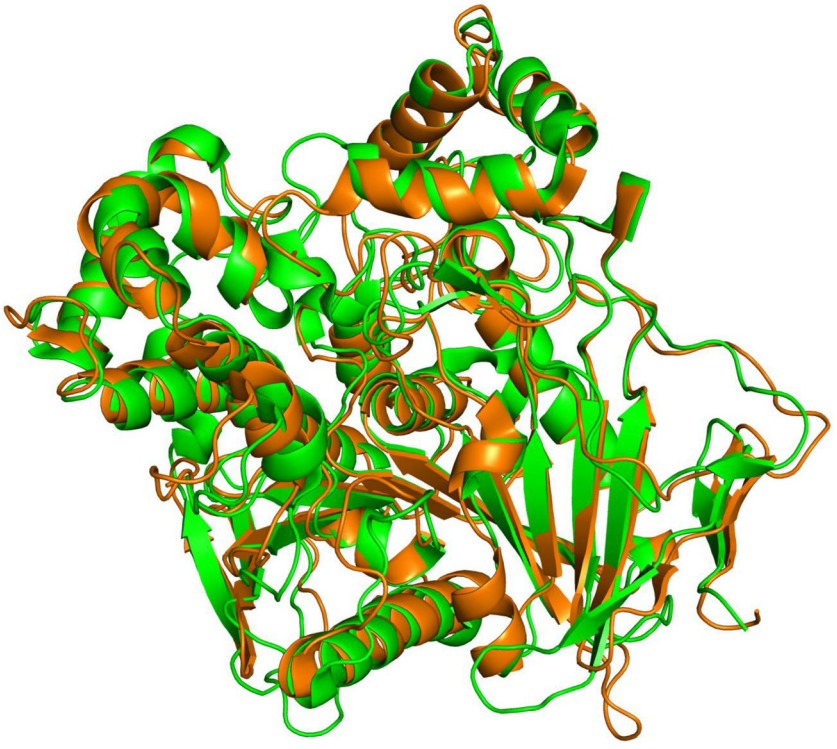

Fig. 4. Crystal structure of EposCCE24 (in green), superimposed with the structure of DmelEst6 (in orange, PDB code 5THM).

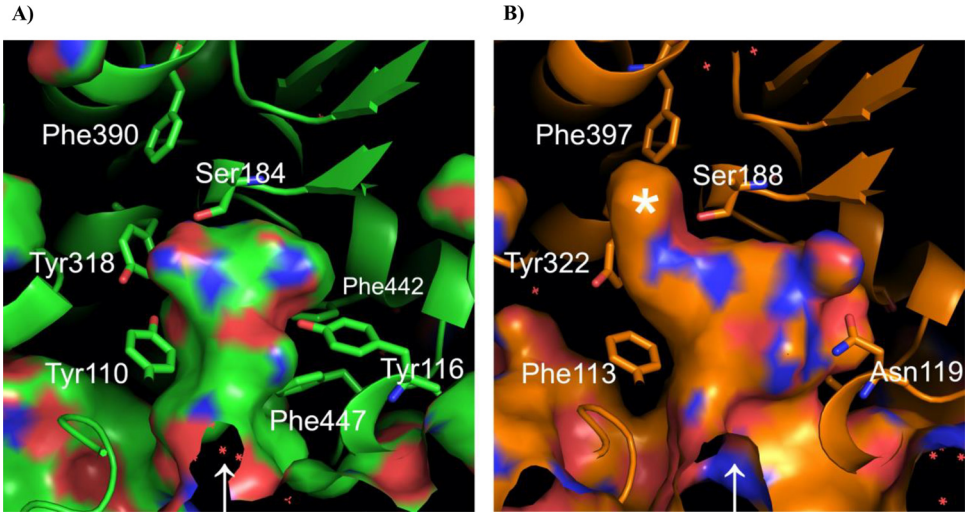

Fig. 5. Comparisons of the internal binding cavities of EposCCE24 (A) and DmelEst6 (B). Polar atoms are shown in red (oxygen) and blue (nitrogen). Key residues lining the binding cavities are shown in stick mode. The white arrows indicate the entrances of the cavities, while the white star indicates the position of the subsite in DmelEst6 (absent in EposCCE24).

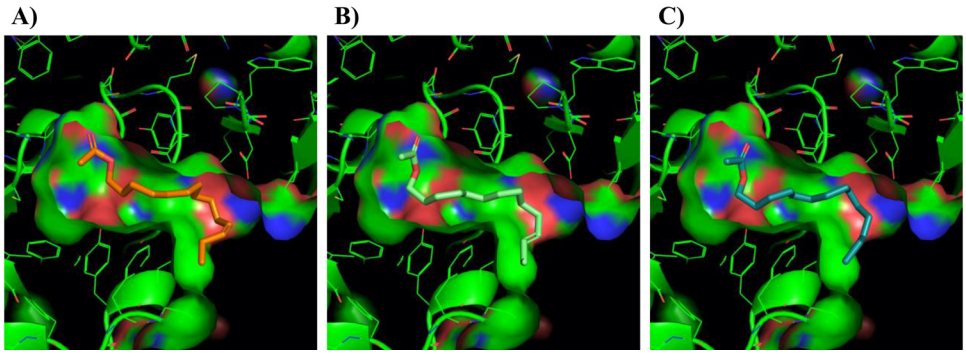

Fig. 6. Docking positions of (A) Z11–14:OAc, (B) E11–14:OAc, and (C) 14:OAc inside the binding cavity of EposCCE24. Compounds are shown in stick mode, with carbon atoms in orange (Z11–14:OAc), green (E11–14:OAc) or teal (14:OAc) and oxygen atoms in red. EposCCE24 carbon atoms are shown in green, while polar atoms are shown in blue (nitrogen) and red (oxygen).

14:OAc) and the related unsaturated compound 14:OAc inside the cavity of EposCCE24 showed that all 3 compounds fit well inside the cavity but can adopt very similar conformations (Fig. 6). Furthermore, due to the length of the cavity, the position of the double bond is predicted to be just around the entrance or slightly outside of the cavity rather than buried (Fig. 6), suggesting that the enzyme may lack the ability to discriminate between these 3 compounds.

3.4. Functional characterization

Recombinant EposCCE24 was evaluated for its ability to hydrolyse 46 volatile, acetate-ester bond-containing lepidopteran sex pheromone components or plant odorants by GC–MS analyses, with a particular focus on acetate-esters due to the structural analysis and their particular biological relevance. In initial screening experiments, all compounds except one, E13–18:OAc, were hydrolysed to some extent by EposCCE24. Generally speaking, smaller (*i.e.*, lower molecular weight or shorter chain length) compounds were hydrolysed faster than bigger compounds, and unsaturated compounds were hydrolysed faster than saturated compounds. No clear pattern was observed with regards to the rate of compound hydrolysis and the location of double bonds within the compounds. Acetate-esters with chain lengths greater than 16 carbon atoms were not hydrolysed efficiently by EposCCE24 (Fig. 7A). In kinetic experiments, the maximum hydrolysis rate (V_{max}) of EposCCE24 for the main sex pheromone component, E11–14:OAc and the behavioural antagonist, Z11–14:OAc, was determined to be 15.28 pM/sec and 26.23 pM/sec, respectively, which equates to a molecular turnover rate of 15.28/sec and 26.23/sec (based on an enzyme concentration of 20 nM in a 50 uL reaction). The measured K_m values of EposCCE24, which are inversely related to the affinity of the enzyme for the substrate were 90.33 and 155.0, for E11–14:OAc and Z11–14:OAc, respectively, indicating the affinity of EposCCE24 was nearly two-fold higher for the main sex pheromone component than it was for the behavioural antagonist (Fig. 7B).

4. Discussion

Depending on the insect, anywhere from several to hundreds of volatile odorant compounds may be biologically relevant, or even critical to its survival. An obvious question, then, is how do insects manage to efficiently metabolise all of these compounds to keep the olfactory system operating? Likewise, how many ODEs does a given insect possess and are these proteins highly specific for individual odorant molecules or are they relatively promiscuous? The current model proposes that the role of ODEs is to clear out non-relevant odorants from the system (that may, perhaps, have some solubility in the aqueous lymph surrounding OSNs), and to remove relevant odorants after they have been delivered to ORs by OBPs (presumably OBPs protect odorants from degradation by ODEs). Since a given insect might express many ODEs in their antennae (*e.g.*, 37 CCEs in *B. mori*), this model supports the hypothesis that ODEs are “tuned” to specific odorant molecules; if ODEs were broadly tuned, relatively few enzymes would be needed to degrade compounds from each chemical class. One valid counter-argument to this reasoning is that ODEs could in fact be broadly tuned, however multiple versions of each class of enzyme are still utilised because they have evolved to be differentially expressed in the various sensilla on the insect antennae. Surprisingly, this does not seem to be the case based on studies that have evaluated sub-antennal expression patterns of ODEs in insects. For example, both *S. exigua* and *S. littoralis* were found to express many ODEs in both male and female antennae, and when the localisation of specific ODEs within the moths’ antennae was evaluated by *in situ* hybridisation experiments, the ODE in question was found to be expressed in multiple

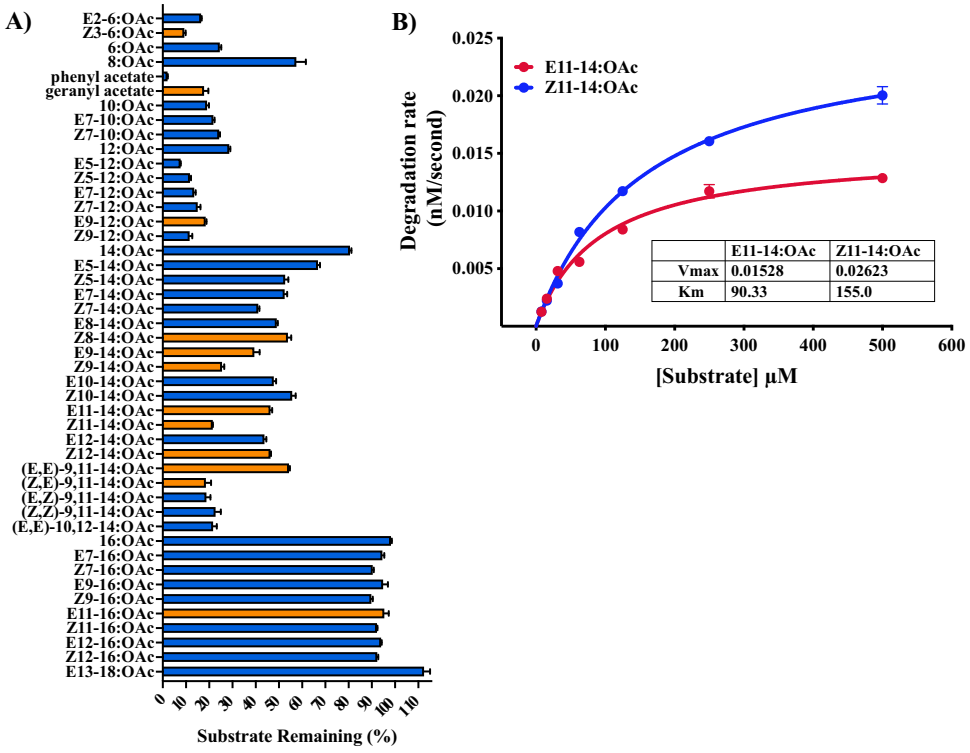

Fig. 7. Degradation of plant volatiles and lepidopteran sex pheromone compounds by recombinant EposCCE24 as determined by GC–MS analyses. A) results from screening experiments, and B) results from kinetic experiments using the behaviourally active compounds, E11–14:OAc and Z11–14:OAc. Results represent the mean (+/- SEM) result from three biological replicates. Orange bars indicate compounds known to elicit electrophysiological responses in *E. postvittana* antennae.

locations within the antennae, including pheromone-detecting sensilla, plant volatile-detecting sensilla, support cells and possibly even OSNs themselves (Durand et al., 2011; He et al., 2015). While limited, these data showing that individual ODEs are not compartmentalised within the insect antennae may support the hypothesis that insect ODEs are tuned to specific odorants; otherwise it is hard to explain why insects would widely express so many ODEs from the same functional class within their antennae.

In this study we aimed to address the question of ODE specificity by focusing on the carboxyl/cholinesterase gene family in the horticultural pest moth, *E. postvittana*. While CCEs are known to have various physiological roles in an organism, the bioinformatic approach used here allowed us to identify 20 CCEs that are likely involved in odorant molecule processing as they are expressed in the insect's antennae and are predicted to be secreted into the sensillar lymph that surrounds olfactory sensory neurons. Following the rationale above, an evolutionary and/or organismal fitness perspective would suggest that each of these individual enzymes are tuned to a specific odorant and the number of these proteins expressed in the antennae more or less represents the number of odorants critical to the moth's survival. Alternatively, these enzymes may in fact be broadly tuned, with overlapping functions, and the expression of 20 different CCE genes in the moth's olfactory organ simply reflects an alternative strategy for improving the rate that acetate-ester odorant molecules are removed from the insect olfactory system.

Of the antennally-expressed carboxylesterases that were identified in this study, we used four key criteria to select one as being a likely "PDE" in this species, and therefore appropriate to address the question of CCE specificity. We prioritised selecting a putative pheromone-degrading CCE based on the reasoning that if any insect CCEs were highly specific for a given compound it would be a pheromone-degrading CCE due to the critical role these molecules have in moth reproduction. The four criteria, in order of importance, were: 1) the presence of a signal peptide on the enzyme's N-terminus, 2) antennally-biased expression, 3) sex-biased antennal expression, and 4) phylogenetic relatedness to other sex pheromone-degrading lepidopteran CCEs. Following these criteria, 10 EposCCEs had signal peptides and displayed antennally-biased expression levels, however none displayed sex-biased antennal expression patterns, in contrast to what has been reported for CCE genes in other moths (Leal et al., 2005; Ishida and Leal 2005; He et al., 2014a; Durand et al., 2011). Following the fourth criterion, five of these 10 EposCCEs (CCEs 01, 12, 14, 17 and 38) were relatively distantly related to any functionally characterised CCEs, three (CCEs 21, 22, and 31) were part of the paralogous expansion event observed in *E. postvittana*, and two (CCEs 15 and 24) were grouped relatively closely to at least some of the lepidopteran CCEs that have been shown to degrade sex pheromone compounds. While it is possible that any of these 10 CCEs are capable of degrading the sex pheromone components used by this species, and that those within the paralogous expansion clade may be of particular importance to this species, we chose to produce recombinant EposCCE24 for structure determination and functional analyses because it was the most closely related *E. postvittana* CCE to the so-called "PDE" from *A. polyphemus* (Ishida and Leal, 2005) as well as to two other lepidopteran CCEs that were shown to degrade sex pheromone compounds.

The size and shape of the binding pocket of EposCCE24 suggested that the enzyme had a preference for linear acetate-esters but didn't have the ability to discriminate between those with varying chain lengths or double bond positions. Indeed, our functional studies validated this hypothesis, as recombinant EposCCE24 was found to hydrolyse linear acetate-esters with hydrocarbon chain lengths ranging from 6 to 16 carbon atoms, with varying double bond positions. Interestingly, while the enzyme hydrolysed all of these compounds, some were hydrolysed more efficiently than others, and two clear patterns were observed: first, shorter-length compounds were hydrolysed more efficiently than longer compounds, and second, compounds of a given length that contained a double bond (or two) were generally hydrolysed more efficiently than saturated compounds of the same length. The catalytic active site of EposCCE24 sits at the end of a narrow tunnel through which the substrates enter, acetate-ester end first, which leaves the long hydrocarbon chain sticking towards the surface or even outside of the enzyme. In absence of structural data of EposCCE24 in complex with either substrates or inhibitors, a mechanistic interpretation of the functional results obtained above remains largely speculative but points towards subtle char-

acteristics of the dynamics of protein-substrate recognition and interactions. For instance, smaller compounds may be hydrolysed faster due to increased stability when fitting completely inside the binding cavity of EposCCE24, compared to larger ones that are partly protruding out. As for the differences observed for saturated *vs* non-saturated and/or cis *vs* trans compounds, they most likely result from the mutual local steric conformations that occur between the protein side chains lining the cavity and the accessible conformational space of the different substrates upon interaction.

The structural and functional data we present here indicate that EposCCE24 is a promiscuous linear acetate-ester-degrading enzyme whose primary role in the olfactory organ is to metabolise odorant molecules in order to keep the olfactory system operating efficiently. While it was found to degrade the main sex pheromone components used by this species, as well as many that are used by other moths, it also degraded various plant-emitted odorant molecules. Because the enzyme's observed specificity is based on the physical properties of the substrate and not the biological role or function of the substrate, we advocate that the term "pheromone degrading enzyme" might be a misnomer. Unlike the relationship between some insect ORs and these same odorant and pheromone compounds, which operate under a lock-and-key model where ORs - especially those that respond to sex pheromones - are thought to be tuned to a specific ligand, here we demonstrate via the structure and function of our best candidate "PDE" that lepidopteran CCEs and odorant molecules do not operate under a similar lock-and-key model. Of course, it is possible that the insight provided into CCE specificity presented here does not hold true for all lepidopteran CCEs, and there may in fact exist highly specific CCEs, including in *E. postvittana*.

The crystal structure of EposCCE24 presented here should more accurately guide future studies in which the substrate specificity of a given lepidopteran CCE is inferred based on the modelling of the enzyme's binding pocket. In addition, this study warrants the inclusion of wide panels of biologically relevant and non-relevant odorant molecules when attempting to characterize the specificity of insect olfactory proteins. Finally, in the absence of any insect ODEs that are highly specific to a particular odorant or pheromone molecule the question remains: why do insects express so many different CCEs (and other ODE classes) in their olfactory organ?

Declaration of Competing Interest

The authors declare that the research was conducted in the absence of any commercial or financial relationships that could be construed as a potential conflict of interest.

CRediT authorship contribution statement

Jacob A. Corcoran: Conceptualization, Funding acquisition, Methodology, Investigation, Formal analysis, Writing – original draft, Writing – review & editing. **Cyril Hamiaux:** Investigation, Formal analysis, Writing – review & editing. **Nicoletta Faraone:** Methodology, Investigation, Formal analysis, Writing – review & editing. **Christer Löfstedt:** Conceptualization, Project administration, Funding acquisition, Writing – review & editing. **Colm Carraher:** Conceptualization, Project administration, Methodology, Investigation, Formal analysis, Writing – review & editing.

Data availability

All raw sequencing data have been deposited in the Sequence Read Archive database at the National Center for Biotechnology Information under BioProject PRJNA976476. The coordinates of EposCCE24 have been deposited in the Protein Data Bank (entry code 7MP4). Open reading frame sequences of EposCCEs are included in supplemental file 1; EposCCE RNAseq readcounts are included in supplementary file 2, and GC-MS data from odorant hydrolysis experiments are included in supplementary file 3.

Acknowledgments

We are very grateful to Jon Agirre (York University) for his help and advice with the refinement of the carbohydrate chains and for supplying unimodal dictionaries for the sugars ahead of their official CCP4 release. The findings and conclusions in this publication are those of the authors and should not be construed to represent any official USDA or U.S. Government determination or policy. Mention of trade names or commercial products in this publication is solely for the purpose of providing specific information and does not imply recommendation or endorsement by the U.S. Department of Agriculture. USDA is an equal opportunity provider and employer.

Funding

This work was supported by the Swedish Foundation for International Cooperation in Research and Higher Education (Grant Nos. IB2013–5256 and IG2013–5483 to C.L), the Swedish Research Council (Vetenskapsrådet, grant number VR-621-2013-4355 to C.L.), the Royal Physiographic Society in Lund (to J.C.), and the U.S. Department of Agriculture, Agricultural Research Service under CRIS project: 5070–22000–038–00D (J.C.).

Supplementary materials

Supplementary material associated with this article can be found, in the online version, at doi:10.1016/j.cris.2023.100062.

References

Andersson, M.N., Newcomb, R.D., 2017. Pest control compounds targeting insect chemoreceptors: another silent spring? Front. Ecol. Evol. 5.
Carey, A.F., Carlson, J.R., 2011. Insect olfaction from model systems to disease control. Proc. Natl. Acad. Sci. U.S.A. 108, 12987–12995.
Chang, H., Liu, Y., Yang, T., Pelosi, P., Dong, S., Wang, G., 2015. Pheromone binding proteins enhance the sensitivity of olfactory receptors to sex pheromones in Chilo suppressalis. Sci. Rep. 5, 13093.
Chertemps, T., Francois, A., Durand, N., Rosell, G., Dekker, T., Lucas, P., Maibeche–Coisne, M., 2012. A carboxylesterase, Esterase-6, modulates sensory physiological and behavioral response dynamics to pheromone in Drosophila. BMC Biol. 10, 56.
Choo, Y.M., Pelletier, J., Atungulu, E., Leal, W.S., 2013. Identification and characterization of an antennae-specific aldehyde oxidase from the navel orangeworm. PLoS One 8, e67794.
Corcoran, J.A., Jordan, M.D., Thrimawithana, A.H., Crowhurst, R.N., Newcomb, R.D., 2015. The peripheral olfactory repertoire of the lightbrown apple moth, epiphyas postvittana. PLoS One 10, e0128596.
Durand, N., Carot-Sans, G., Chertemps, T., Bozzolan, F., Party, V., Renou, M., Debernard, S., Rosell, G., Maibeche-Coisne, M., 2010. Characterization of an antennal carboxylesterase from the pest moth Spodoptera littoralis degrading a host plant odorant. PLoS One 5, e15026.
Durand, N., Carot-Sans, G., Bozzolan, F., Rosell, G., Siaussat, D., Debernard, S., Chertemps, T., Maibeche-Coisne, M., 2011. Degradation of pheromone and plant volatile components by a same odorant-degrading enzyme in the cotton leafworm, spodoptera littoralis. PLoS One 6, e29147.
Durand, N., Chertemps, T., Maibeche-Coisne, M., 2012. Antennal carboxylesterases in a moth, structural and functional diversity. Commun. Integr. Biol. 5, 284–286.
El-Sayed, A.M., Mitchell, V.J., Manning, L.A.M., Suckling, D.M., 2011. New sex pheromone blend for the lightbrown apple moth, epiphyas postvittana. J. Chem. Ecol. 37, 640–646.
Emsley, P., Lohkamp, B., Scott, W.G., Cowtan, K., 2010. Features and development of Coot. Acta Crystallogr. D Biol. Crystallogr. 66, 486–501.
Evans, P.R., Murshudov, G.N., 2013. How good are my data and what is the resolution? Acta Crystallogr. D Biol. Crystallogr. 69, 1204–1214.
Forstner, M., Breer, H., Krieger, J., 2009. A receptor and binding protein interplay in the detection of a distinct pheromone component in the silkmoth Antheraea polyphemus. Int. J. Biol. Sci. 5, 745–757.
Grabherr, M.G., Haas, B.J., Yassour, M., Levin, J.Z., Thompson, D.A., Amit, I., Adiconis, X., Fan, L., Raychowdhury, R., Zeng, Q., Chen, Z., Mauceli, E., Hacohen, N., Gnirke, A., Rhind, N., Di Palma, F., Birren, B.W., Nusbaum, C., Lindblad-Toh, K., Friedman, N., Regev, A., 2011. Full-length transcriptome assembly from RNA-Seq data without a reference genome. Nat. Biotechnol. 29, 644–652.
Han, Q., Wong, D.M., Robinson, H., Ding, H., Lam, P.C.H., Totrov, M.M., Carlier, P.R., Li, J., 2018. Crystal structure of acetylcholinesterase catalytic subunits of the malaria vector Anopheles gambiae. Insect Sci. 25, 721–724.

Harel, M., Kryger, G., Rosenberry, T.L., Mallender, W.D., Lewis, T., Fletcher, R.J., Guss, J.M., Silman, I., Sussman, J.L., 2000. Three-dimensional structures of drosophila melanogaster acetylcholinesterase and of its complexes with two potent inhibitors. Protein Sci. 9, 1063–1072.

He, P., Li, Z.Q., Liu, C.C., Liu, S.J., Dong, S.L., 2014a. Two esterases from the genus Spodoptera degrade sex pheromones and plant volatiles. Genome 57, 201–208.

He, P., Zhang, J., Li, Z.Q., Zhang, Y.N., Yang, K., Dong, S.L., He, P., 2014b. Functional characterization of an antennal esterase from the noctuid moth, Spodoptera exigua. Arch. Insect Biochem. Physiol. 86, 85–99.

He, P., Zhang, Y.N., Li, Z.Q., Yang, K., Zhu, J.Y., Liu, S.J., Dong, S.L., 2014c. An antennae-enriched carboxylesterase from Spodoptera exigua displays degradation activity in both plant volatiles and female sex pheromones. Insect Mol. Biol. 23, 475–486.

He, P., Zhang, Y.N., Yang, K., Li, Z.Q., Dong, S.L., 2015. An antenna-biased carboxylesterase is specifically active to plant volatiles in Spodoptera exigua. Pestic. Biochem. Physiol. 123, 93–100.

He, P., Mang, D.Z., Wang, H., Wang, M.M., Ma, Y.F., Wang, J., Chen, G.L., Zhang, F., He, M., 2020. Molecular characterization and functional analysis of a novel candidate of cuticle carboxylesterase in Spodoptera exigua degradating sex pheromones and plant volatile esters. Pestic. Biochem. Physiol. 163, 227–234.

Hopkins, D.H., Fraser, N.J., Mabbitt, P.D., Carr, P.D., Oakeshott, J.G., Jackson, C.J., 2017. Structure of an insecticide sequestering carboxylesterase from the disease vector culex quinquefasciatus: what makes an enzyme a good insecticide sponge? Biochemistry 56, 5512–5525.

Ishida, Y., Leal, W.S., 2002. Cloning of putative odorant-degrading enzyme and integumental esterase cDNAs from the wild silkmoth, antheraea polyphemus. Insect Biochem. Mol. Biol. 32, 1775–1780.

Ishida, Y., Leal, W.S., 2005. Rapid inactivation of a moth pheromone. Proc. Natl. Acad. Sci. U. S. A. 102, 14075–14079.

Jackson, C.J., Liu, J.W., Carr, P.D., Younus, F., Coppin, C., Meirelles, T., Lethier, M., Pandey, G., Ollis, D.L., Russell, R.J., Weik, M., Oakeshott, J.G., 2013. Structure and function of an insect alpha-carboxylesterase (alphaEsterase7) associated with insecticide resistance. Proc. Natl. Acad. Sci. U. S. A. 110, 10177–10182.

Jordan, M.D., Stanley, D., Marshall, S.D.G., De Silva, D., Crowhurst, R.N., Gleave, A.P., Greenwood, D.R., Newcomb, R.D, 2008. Expressed sequence tags and proteomics of antennae from the tortricid moth, Epiphyas postvittana. Insect Mol. Biol. 17, 361–373.

Kabsch, W., 2010. Xds. Acta. Crystallogr. D Biol. Crystallogr. 66, 125–132.

Leal, J.F., Barbancho, M., 1993. Aldehyde dehydrogenase (ALDH) activity in Drosophila melanogaster adults: evidence for cytosolic localization. Insect Biochem. Mol. Biol. 23, 543–547.

Leal, W.S., Chen, A.M., Ishida, Y., Chiang, V.P., Erickson, M.L., Morgan, T.I., Tsuruda, J.M., 2005. Kinetics and molecular properties of pheromone binding and release. Proc. Natl. Acad. Sci. U.S.A. 102, 5386–5391.

Leal, W.S., 2013. Odorant reception in insects: roles of receptors, binding proteins, and degrading enzymes. Annu. Rev. Entomol. 58, 373–391.

Li, B., Dewey, C.N., 2011. RSEM: accurate transcript quantification from RNA-Seq data with or without a reference genome. BMC Bioinf. 12, 323.

Liebschner, D., Afonine, P.V., Baker, M.L., Bunkoczi, G., Chen, V.B., Croll, T.I., Hintze, B., Hung, L.W., Jain, S., Mccoy, A.J., Moriarty, N.W., Oeffner, R.D., Poon, B.K., Prisant, M.G., Read, R.J., Richardson, J.S., Richardson, D.C., Sammito, M.D., Sobolev, O.V., Stockwell, D.H., Terwilliger, T.C., Urzhumtsev, A.G., Videau, L.L., Williams, C.J., Adams, P.D., 2019. Macromolecular structure determination using X-rays, neutrons and electrons: recent developments in Phenix. Acta Crystallogr. D Struct. Biol. 75, 861–877.

Love, M.I., Huber, W., Anders, S., 2014. Moderated estimation of fold change and dispersion for RNA-seq data with DESeq2. Genome Biol. 15, 550.

Maibeche-Coisne, M., Nikonov, A.A., Ishida, Y., Jacquin-Joly, E., Leal, W.S., 2004a. Pheromone anosmia in a scarab beetle induced by *in vivo* inhibition of a pheromone-degrading enzyme. Proc. Natl. Acad. Sci. U. S. A. 101, 11459–11464.

Maibeche-Coisne, M., Merlin, C., Francois, M.C., Queguiner, I., Porcheron, P., Jacquin-Joly, E., 2004b. Putative odorant-degrading esterase cDNA from the moth Mamestra brassicae: cloning and expression patterns in male and female antennae. Chem. Senses 29, 381–390.

Merlin, C., Rosell, G., Carot-Sans, G., Francois, M.C., Bozzolan, F., Pelletier, J., Jacquin-Joly, E., Guerrero, A., Maibeche-Coisne, M., 2007. Antennal esterase cDNAs from two pest moths, spodoptera littoralis and Sesamia nonagrioides, potentially involved in odourant degradation. Insect Mol. Biol. 16, 73–81.

Morris, G.M., Huey, R., Lindstrom, W., Sanner, M.F., Belew, R.K., Goodsell, D.S., Olson, A.J., 2009. AutoDock4 and AutoDockTools4: automated docking with selective receptor flexibility. J. Comput. Chem. 30, 2785–2791.

Murshudov, G.N., Skubak, P., Lebedev, A.A., Pannu, N.S., Steiner, R.A., Nicholls, R.A., Winn, M.D., Long, F., Vagin, A.A., 2011. REFMAC5 for the refinement of macromolecular crystal structures. Acta. Crystallogr. D Biol. Crystallogr. 67, 355–367.

O'boyle, N.M., Banck, M., James, C.A., Morley, C., Vandermeersch, T., Hutchison, G.R., 2011. Open Babel: an open chemical toolbox. J. Cheminformatics 3, 33.

Qiu, C.Z., Zhou, Q.Z., Liu, T.T., Fang, S.M., Wang, Y.W., Fang, X., Huang, C.L., Yu, Q.Y., Chen, C.H., Zhang, Z., 2018. Evidence of peripheral olfactory impairment in the domestic silkworms: insight from the comparative transcriptome and population genetics. BMC Genomics 19, 788 [Electronic Resource].

Roh, G.H., Park, K.C., 2022. Electrophysiological and behavioral activities of sex pheromone and structurally related compounds in lightbrown apple moth, epiphyas postvittana. Chemoecology 32, 1–13.

Suckling, D.M., Karg, G., Gibb, A.R., Bradley, S.J., 1996. Electroantennogram and oviposition responses of Epiphyas postvittana (Lepidoptera: tortricidae) to plant volatiles. N. Z. J. Crop Hortic. Sci. 24, 323–333.

Tooman, L.K., Rose, C.J., Carraher, C., Suckling, D.M., Paquette, S.R., Ledezma, L.A., Gilligan, T.M., Epstein, M., Barr, N.B., Newcomb, R.D., 2011. Patterns of mitochondrial haplotype diversity in the invasive pest Epiphyas postvittana (Lepidoptera: tortricidae). J. Econ. Entomol. 104, 920–932.

Trott, O., Olson, A.J., 2010. AutoDock Vina: improving the speed and accuracy of docking with a new scoring function, efficient optimization, and multithreading. J. Comput. Chem. 31, 455–461.

Vagin, A., Lebedev, A., 2015. MoRDa, an automatic molecular replacement pipeline. Acta Crystallogr. Sect. A 71, s19.

Venthur, H., Zhou, J.J., 2018. Odorant receptors and odorant-binding proteins as insect pest control targets: a comparative analysis. Front. Physiol. 9.

Vogt, R.G., 2005. Molecular Basis of Pheromone Detection in Insects. Elsevier, London.

Walker 3rd, W.B., Roy, A., Anderson, P., Schlyter, F., Hansson, B.S., Larsson, M.C., 2019. Transcriptome analysis of gene families involved in chemosensory function in spodoptera littoralis (Lepidoptera: noctuidae). BMC Genom. 20, 428 [Electronic Resource].

Winn, M.D., Ballard, C.C., Cowtan, K.D., Dodson, E.J., Emsley, P., Evans, P.R., Keegan, R.M., Krissinel, E.B., Leslie, A.G., Mccoy, A., Mcnicholas, S.J., Murshudov, G.N., Pannu, N.S., Potterton, E.A., Powell, H.R., Read, R.J., Vagin, A., Wilson, K.S., 2011. Overview of the CCP4 suite and current developments. Acta. Crystallogr. D Biol. Crystallogr. 67, 235–242.

Wogulis, M., Wheelock, C.E., Kamita, S.G., Hinton, A.C., Whetstone, P.A., Hammock, B.D., Wilson, D.K., 2006. Structural studies of a potent insect maturation inhibitor bound to the juvenile hormone esterase of Manduca sexta. Biochemistry 45, 4045–4057.

Xu, P., Atkinson, R., Jones, D.N., Smith, D.P., 2005. Drosophila OBP LUSH is required for activity of pheromone-sensitive neurons. Neuron 45, 193–200.

Younus, F., Chertemps, T., Pearce, S.L., Pandey, G., Bozzolan, F., Coppin, C.W., Russell, R.J., Maibeche-Coisne, M., Oakeshott, J.G., 2014. Identification of candidate odorant degrading gene/enzyme systems in the antennal transcriptome of Drosophila melanogaster. Insect Biochem. Mol. Biol. 53, 30–43.

Younus, F., Fraser, N.J., Coppin, C.W., Liu, J.W., Correy, G.J., Chertemps, T., Pandey, G., Maibeche, M., Jackson, C.J., Oakeshott, J.G., 2017. Molecular basis for the behavioral effects of the odorant degrading enzyme esterase 6 in drosophila. Sci. Rep. 7, 46188.